Manganese−Group 11 Element and −Zinc Mixed-Metal Clusters Derived from the Binuclear Dianion $[Mn_2\{\mu\text{-}P(OEt)_2\}\{\mu\text{-}\eta^2\text{-}OP(OEt)_2\}(CO)_6]^{2-}$. X-ray Structures of $[Mn_2Zn\{\mu\text{-}P(OEt)_2\}\{\mu\text{-}\eta^2\text{-}OP(OEt)_2\}(CO)_6(C_{10}H_8N_2\text{-}N,N')]$ and $[Mn_2Au_3\{\mu\text{-}P(OEt)_2\}(CO)_6(PPh_3)_3]$

Xiang-Yang Liu, Victor Riera,* and Miguel A. Ruiz

Instituto de Química Organometálica, Universidad de Oviedo, E-33071 Oviedo, Spain

Antonio Tiripicchio and Marisa Tiripicchio-Camellini

Dipartimento di Chimica Generale ed Inorganica, Chimica Analitica, Chimica Fisica, Centro di Studio per la Strutturistica Diffrattometrica del CNR, Università di Parma, Viale delle Scienze 78, I-43100 Parma, Italy

Received August 2, 1995[⊗]

The binuclear dianion $[Mn_2\{\mu\text{-}P(OEt)_2\}\{\mu\text{-}\eta^2\text{-}OP(OEt)_2\}(CO)_6]^{2-}$ (as the Na^+ salt) reacts readily in tetrahydrofuran at room temperature with the chloro complexes $[ZnCl_2(bpy)]$ or $[MCl(PR_3)]_n$ (bpy = $C_{10}H_8N_2$-*N*,*N*′; M = Au, Cu, R = Ph, Et; M = Ag, R = Ph) to give the corresponding trinuclear clusters $[Mn_2Zn\{\mu\text{-}P(OEt)_2\}\{\mu\text{-}\eta^2\text{-}OP(OEt)_2\}(CO)_6(bpy)]$ or $Na[Mn_2M\{\mu\text{-}P(OEt)_2\}\{\mu\text{-}\eta^2\text{-}OP(OEt)_2\}(CO)_6(PR_3)]$ in high yield. The latter have been isolated as the corresponding tetraphenylarsonium salts after ion exchange with $[AsPh_4]Cl$ in dichloromethane. The trinuclear anions (as Na^+ salts) react with a second equivalent of $[MCl(PR_3)]_n$ in toluene, but the expected tetranuclear clusters $[Mn_2M_2\{\mu\text{-}P(OEt)_2\}\{\mu\text{-}\eta^2\text{-}OP(OEt)_2\}(CO)_6(PR_3)_2]$ are formed only for M = Au, Ag and have a low thermal stability. In the case of copper, electron transfer rather than metal−metal bond formation occurs. Decomposition of the digold manganese clusters in the presence of $[AuCl(PR_3)]$ gives the unsaturated pentanuclear clusters $[Mn_2Au_3\{\mu\text{-}P(OEt)_2\}(CO)_6(PR_3)_3]$ (R = Ph, Et) in low yields (10−15% at best). The structure of the latter (**8a**; R = Ph) and that of the dimanganese zinc cluster (**2**) have been determined by X-ray diffraction methods. The structures of the new compounds as well as the dynamic behavior or ion-pairing effects in some of them are discussed on the basis of the IR and NMR (^1H, ^{31}P) data. It is concluded that the ^{31}P chemical shift of the bridging diethoxyphosphido ligand in these and related manganese systems cannot be used as a reliable probe for the presence of a manganese−manganese bond.

Introduction

The chemistry of heteronuclear clusters of the transition metals remains an active area of research.[1] In addition to the strong interest in the structure, bonding, and reactivity of these species, increasing attention is being paid to their catalytic behavior and possible connections (as models or precursors) with heterometallic alloy catalysts. Rational syntheses for these molecules require selective metal−metal bond formation steps, which can be accomplished, *inter alia*, through the reaction of transition-metal carbonyl anions with suitable halogeno complexes or related species.

Recently[2] we have reported the synthesis and oxidation reactions of the binuclear dianion $[Mn_2\{\mu\text{-}P(OEt)_2\}\{\mu\text{-}\eta^2\text{-}OP(OEt)_2\}(CO)_6]^{2-}$ (**1**; Na^+ salt), unexpectedly formed through Na amalgam reduction of the unsaturated hydride $[Mn_2(\mu\text{-}H)_2\{\mu\text{-}(EtO)_2POP(OEt)_2\}(CO)_6]$.[3] The presence of two negative charges and two robust bridging groups in **1** should make this anion a suitable precursor for the rational synthesis of tri- and tetranuclear heterometallic clusters. On the other hand, heteronuclear manganese clusters are relatively rare species.[1] We therefore decided to examine the reactions of **1** with several halogeno complexes. No reaction or electron transfer,[2] rather than metal−metal bond formation, occurred when treating **1** with early- or middle-transition-metal halogeno complexes such as $[TiCl_2Cp_2]$, $[MClCp(CO)_3]$ (M = Mo, W), $[MnBr(CO)_5]$, or $[FeBr(\eta^3\text{-}C_3H_5)(CO)_3]$. Metal−metal bond formation, however, occurred when using group 11 element or zinc halogeno complexes. As will be next discussed, these reactions allow the synthesis of clusters having Mn_2M (M = Zn, Cu, Ag, Au), Mn_2M_2 (M = Ag, Au), or Mn_2Au_3 metal cores. While some compounds with Mn_2M (M = Cu, Ag, Au, Zn, Hg) skeletons had been previously reported by

[⊗] Abstract published in *Advance ACS Abstracts,* December 15, 1995.

(1) Reviews: (a) Robert, D. A.; Geoffroy, G. L. In *Comprehensive Organometallic Chemistry*; Wilkinson, G., Stone, F. G. A., Abel, E. W., Eds.; Pergamon: Oxford, U.K., 1982; Vol. 6, Chapter 40. (b) Stephan, D. W. *Coord. Chem. Rev.* **1989**, *95*, 41. (c) Gomes Carneiro, T. M.; Matt, D.; Braunstein, P. *Coord. Chem. Rev.* **1989**, *96*, 49. (d) Salter, I. D. *Adv. Organomet. Chem.* **1989**, *29*, 249. (e) Farrugia, L. J. *Adv. Organomet. Chem.* **1989**, *31*, 301. (f) Mingos, D. M. P.; Watson, M. J. *Adv. Inorg. Chem.* **1992**, *39*, 327.

(2) Liu, X.-Y.; Riera, V.; Ruiz, M. A.; Lanfranchi, M.; Tiripicchio, A.; Tiripicchio-Camellini, M. *Organometallics* **1994**, *13*, 1940.

(3) This reaction was originally thought to give the unsaturated anion $[Mn_2(CO)_6\{\mu\text{-}(EtO)_2POP(OEt)_2\}]^{2-}$. See: Ruiz, M. A.; Riera, V.; Tiripicchio, A.; Tiripicchio-Camellini, M. *J. Chem. Soc., Chem. Commun.* **1985**, 1505. The tentative formulation of some $M(PPh_3)$ (M = Cu, Ag, Au) derivatives made there was also erroneous.

0276-7333/96/2315-0974$12.00/0

Table 1. IR Data for New Compounds[a]

compd	ν(CO)[b]/cm^{-1}
$Na_2[Mn_2\{\mu\text{-}P(OEt)_2\}\{\mu\text{-}OP(OEt)_2\}(CO)_6]$ (**1**)	1959 (s), 1901 (vs), 1857 (s), 1834 (s), 1819 (s), 1786 (w, sh)[a,c]
$[Mn_2Zn\{\mu\text{-}P(OEt)_2\}\{\mu\text{-}OP(OEt)_2\}(CO)_6(bpy)]$ (**2**)	1998 (w), 1970 (vs), 1922 (s), 1888 (s), 1862 (m)[d]
$Na[Mn_2Au\{\mu\text{-}P(OEt)_2\}\{\mu\text{-}OP(OEt)_2\}(CO)_6(PPh_3)]$ (**3a**) (Na^+ salt)	1980 (w), 1948 (vs), 1900 (s), 1874 (s), 1859 (m, sh)[c]
$[AsPh_4][Mn_2Au\{\mu\text{-}P(OEt)_2\}\{\mu\text{-}OP(OEt)_2\}(CO)_6(PPh_3)]$ (**3a**)	1969 (m), 1937 (vs), 1875 (s, br)
$[AsPh_4][Mn_2Au\{\mu\text{-}P(OEt)_2\}\{\mu\text{-}OP(OEt)_2\}(CO)_6(PEt_3)]$ (**3b**)	1967 (w), 1934 (vs), 1872 (s, sh), 1864 (s)
$Na[Mn_2Ag\{\mu\text{-}P(OEt)_2\}\{\mu\text{-}OP(OEt)_2\}(CO)_6(PPh_3)]$ (**4**) (Na^+ salt)	1974 (m), 1938 (vs), 1892 (s), 1867 (s), 1857 (m, sh)[c]
$[AsPh_4][Mn_2Ag(\mu\text{-}P(OEt)_2\}\{\mu\text{-}OP(OEt)_2\}(CO)_6(PPh_3)]$ (**4**)	1964 (w), 1926 (vs), 1863 (s, br)
$Na[Mn_2Cu\{\mu\text{-}P(OEt)_2\}\{\mu\text{-}OP(OEt)_2\}(CO)_6(PPh_3)]$ (**5a**) (Na^+ salt)	1975 (m), 1936 (vs), 1891 (s), 1867 (s), 1857 (m, sh)[c]
$[AsPh_4][Mn_2Cu\{\mu\text{-}P(OEt)_2\}\{\mu\text{-}OP(OEt)_2\}(CO)_6(PPh_3)]$ (**5a**)	1964 (w), 1924 (vs), 1867 (s), 1855 (s, sh)
$[AsPh_4][Mn_2Cu\{\mu\text{-}P(OEt)_2\}\{\mu\text{-}OP(OEt)_2\}(CO)_6(PEt_3)]$ (**5b**)	1962 (w), 1921 (vs), 1865 (s), 1850 (s, br)
$[Mn_2Au_2\{\mu\text{-}P(OEt)_2\}\{\mu\text{-}OP(OEt)_2\}(CO)_6(PPh_3)_2]$ (**6**)	1992 (w), 1969 (vs), 1915 (s), 1889 (m), 1865 (w, sh)[e]
$[Mn_2Ag_2\{\mu\text{-}P(OEt)_2\}\{\mu\text{-}OP(OEt)_2\}(CO)_6(PPh_3)_2]$ (**7**)	1989 (w), 1963 (vs), 1904 (s), 1874 (m), 1859 (w)[e]
$[Mn_2Au_3\{\mu\text{-}P(OEt)_2\}(CO)_6(PPh_3)_3]$ (**8a**)	1961 (w), 1935 (vs), 1889 (s), 1858 (m)[e]
$[Mn_2Au_3\{\mu\text{-}P(OEt)_2\}(CO)_6(PEt_3)_3]$ (**8b**)	1960 (w), 1936 (vs), 1887 (s), 1853 (m)[f]

[a] Data for compound **1** taken from ref 2. [b] Recorded in dichloromethane solution, unless otherwise stated. [c] In tetrahydrofuran solution. [d] In diethyl ether solution. [e] In toluene solution. [f] In petroleum ether solution.

Chart 1

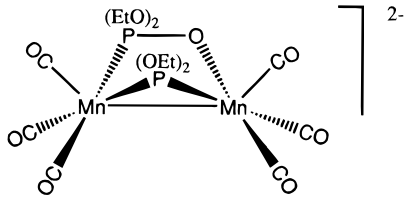

1

us[4−7] and others,[8] the first examples of complexes having Mn_2Au_2 or Mn_2Au_3 cores have only appeared while our work was in progress.[9]

Results and Discussion

Trinuclear Derivatives. From a structural point of view, anion **1** can be related to the well-known complexes of formula $[Fe_2(\mu\text{-}X)_2(CO)_6]$ (X = halide, phosphido, thiolato, and related 4e-donor ligands), which are isoelectronic with **1**. The IR spectrum of **1** in the ν_{st}(CO) region (Table 1)[2] exhibits a pattern very similar to that found for the above-mentioned diiron species,[10] and thus a similar structure is assumed for **1** (Chart 1). Therefore, it is relatively straightforward to anticipate that the coordinatively unsaturated cationic metal fragment ML_n^{x+} should be able to bind the dimanganese center of anion **1** at the "pocket" position of the molecule. In order to get neutral derivatives, we first examined the reactions of **1** toward group 12 halogeno derivatives.

Anion **1** reacts readily with $[ZnCl_2(bpy)]$ (bpy = 2,2′-bipyridine) at room temperature to afford the red neutral cluster $[Mn_2Zn\{\mu\text{-}P(OEt)_2\}\{\mu\text{-}\eta^2\text{-}OP(OEt)_2\}(CO)_6(bpy)]$ (**2**) in high yield. The IR spectrum of **2** exhibits a ν_{st}(CO) pattern similar to that of **1** but shifted considerably toward higher frequencies, as expected.

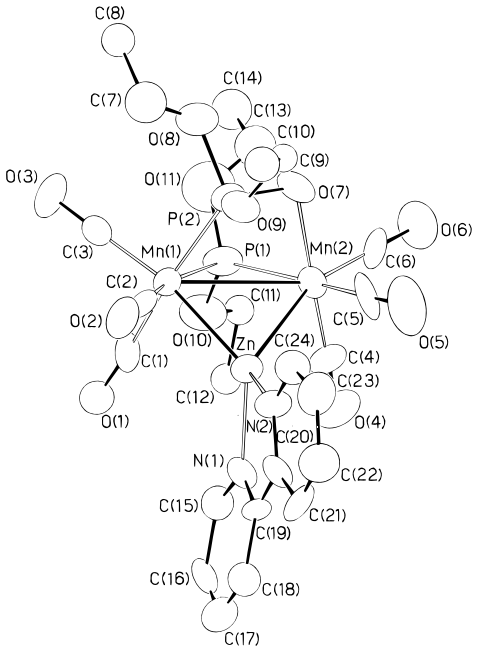

Figure 1. Molecular structure of **2**, with the atom-numbering scheme.

This suggests a small structural reorganization of the dimanganese moiety upon cluster formation.

The molecular structure of **2** has been fully elucidated by X-ray diffraction methods and is shown in Figure 1 together with the atom-numbering scheme. Selected bond distances and angles are given in Table 2.

In the molecule the two $Mn(CO)_3$ units are triply bridged by the diethoxyphosphido ligand through the P(1) atom, by the diethylphosphonate ligand through the P(2) and O(7) atoms, and by the (bipyridine)zinc group through the Zn atom.

The Mn−P bond distances involving the phosphido (Mn(1)−P(1) = 2.226(6) Å and Mn(2)−P(1) = 2.219(8) Å) or phosphonate (Mn(1)−P(2) = 2.227(8) Å) ligands are significantly shorter (by *ca.* 0.06−0.13 Å) than in the complexes $[Mn_2\{\mu\text{-}P(OEt)_2\}\{\mu\text{-}\eta^2\text{-}OP(OEt)_2\}(CO)_xL]$ (L = PPh_3, x = 7; L = $Me_2PCH_2PMe_2$, x = 6),[2] as expected for a dimetallic moiety with a lower electron density (fewer ligands around manganese, lower ν_{st}(CO) frequencies). Somewhat unexpectedly, the P(1) phosphido atom in **2** bridges the manganese centers in an almost symmetrical fashion, so it cannot counterbalance the intrinsic asymmetry of the phosphonate group.[2] In contrast, the Mn−O bond distance involving the phos-

(4) Riera, V.; Ruiz, M. A.; Tiripicchio, A.; Tiripicchio-Camellini, M. *J. Chem. Soc., Dalton Trans.* **1987**, 1551.
(5) Carreño, R.; Riera, V.; Ruiz, M. A.; Bois, C.; Jeannin, Y. *Organometallics* **1992**, *11*, 2923.
(6) Riera, V.; Ruiz, M. A.; Tiripicchio, A.; Tiripicchio-Camellini, M. *Organometallics* **1993**, *12*, 2962.
(7) Carreño, R.; Riera, V.; Ruiz, M. A.; Tiripicchio, A.; Tiripicchio-Camellini, M. *Organometallics* **1994**, *13*, 993.
(8) (a) Iggo, J. A.; Mays, M. J.; Raithby, P. R.; Henrick, K. *J. Chem. Soc., Dalton Trans.* **1984**, 633. (b) Iggo, J. A.; Mays, M. J. *J. Chem. Soc., Dalton Trans.* **1984**, 643.
(9) Haupt, H. J.; Heinekamp, C.; Flörke, U.; Juptner, U. *Z. Anorg. Allg. Chem.* **1992**, *608*, 100.
(10) Bor, G. *J. Organomet. Chem.* **1975**, *94*, 181.

Table 2. Selected Bond Distances (Å) and Angles (deg) in Complex 2

Zn−Mn(1)	2.450(5)	P(1)−O(10)	1.618(18)
Zn−Mn(2)	2.544(4)	P(1)−O(11)	1.660(20)
Zn−N(1)	2.074(20)	P(2)−O(7)	1.503(15)
Zn−N(2)	2.074(18)	P(2)−O(8)	1.66(2)
Mn(1)−Mn(2)	2.914(5)	P(2)−O(9)	1.617(15)
Mn(1)−P(1)	2.226(6)	Mn(2)−P(1)	2.219(8)
Mn(1)−P(2)	2.227(8)	Mn(2)−O(7)	2.075(16)
Mn(1)−C(1)	1.74(2)	Mn(2)−C(4)	1.71(3)
Mn(1)−C(2)	1.80(2)	Mn(2)−C(5)	1.76(2)
Mn(1)−C(3)	1.76(2)	Mn(2)−C(6)	1.68(2)
N(1)−Zn−N(2)	80.0(7)	Mn(1)−Zn−Mn(2)	71.4(1)
Zn−Mn(1)−C(2)	72.8(7)	Zn−Mn(2)−C(5)	77.1(8)
Zn−Mn(1)−C(1)	81.9(8)	Zn−Mn(2)−C(4)	74.3(9)
Zn−Mn(1)−P(2)	93.3(2)	Zn−Mn(2)−O(7)	108.6(4)
Zn−Mn(1)−P(1)	94.9(2)	Zn−Mn(2)−P(1)	92.5(2)
P(2)−Mn(1)−C(1)	173.8(8)	O(7)−Mn(2)−C(4)	177.0(10)
P(2)−Mn(1)−C(2)	87.8(8)	O(7)−Mn(2)−C(6)	88.0(10)
P(2)−Mn(1)−C(3)	94.9(7)	O(7)−Mn(2)−C(5)	85.9(9)
P(1)−Mn(1)−C(3)	93.4(7)	P(1)−Mn(2)−C(6)	100.2(9)
P(1)−Mn(1)−C(2)	165.7(7)	P(1)−Mn(2)−C(5)	164.2(8)
P(1)−Mn(1)−P(2)	85.7(3)	P(1)−Mn(2)−O(7)	86.2(5)
Mn(2)−Mn(1)−C(2)	116.8(6)	Mn(1)−Mn(2)−C(5)	115.5(8)
Mn(2)−Mn(1)−C(1)	110.3(8)	Mn(1)−Mn(2)−C(4)	105.1(8)
Mn(2)−Mn(1)−P(2)	63.7(2)	Mn(1)−Mn(2)−O(7)	76.5(4)
Mn(1)−P(1)−Mn(2)	81.9(3)	Mn(1)−P(2)−O(7)	114.4(7)

phonate ligand (Mn(2)−O(7) = 2.075(16) Å) is comparable to those found in the already cited complexes (2.069(4) and 2.059(6) Å).[2] As the oxygen donor atom of the phosphonate ligand is a poorer electron donor than phosphorus, we expect the corresponding manganese atom (Mn(2)) to be electron poorer than that bearing the P end of the ligand (Mn(1)). As a result, the latter metal atom should bind the cationic [Zn(bpy)] fragment in a stronger way, in agreement with the observed Mn−Zn distances (Mn(1)−Zn = 2.450(5) Å and Mn(2)−Zn = 2.544(4) Å). The longer Mn−Zn distance in **2** is comparable to those found in the complex $[Mn_2Zn(\mu\text{-}H)_2(CO)_6(Me_2NCH_2CH_2NMe_2)\{\mu\text{-}(EtO)_2POP(OEt)_2\}]$, 2.525(4) and 2.544(4) Å,[6] which still seems to be the only other Mn−Zn cluster characterized by X-ray diffraction methods so far, and where the values of these distances are influenced by the presence of the bridging hydrides.[11] Overall, the Mn−Zn distances in **2** should be taken as indicative of fairly strong bonding interactions in the metal core due to the high acidity of the zinc fragment. This is also shown by the relatively short Mn(1)−Mn(2) distance, 2.914(5) Å, which is normal for a single bond between manganese atoms (for example, it is 2.9038(6) Å in $[Mn_2(CO)_{10}]$[12]), even if it is substantially shorter than that found for the above-mentioned hydrido cluster (3.039(5) Å))[6] or those observed in trimetallic Mn_2Au clusters (*ca.* 3.07−3.09 Å)[4,8a,9] which incorporate the fragment $[Au(PR)_3]^+$, electronically related to the (bipyridine)zinc(II) moiety.

In an attempt to prepare Mn_2Hg clusters related to **2**, we investigated the reactions of **1** with HgI_2, either itself or in the presence of phosphines. In all cases, a deep green solution is rapidly formed at −78 °C. However, when the temperature is raised above *ca.* −50 °C, yellow-orange solutions are quickly formed. The latter solutions were shown (by IR and ^{31}P NMR spectroscopy) to contain the same products formed when 2 equiv of $[FeCp_2]PF_6$ is used instead of HgI_2.[2] Then,

(11) Teller, R. G.; Bau, R. *Struct. Bonding* **1981**, *44*, 1.
(12) Churchill, M. R.; Amoh, K. N.; Wassermann, H. J. *Inorg. Chem.* **1981**, *20*, 1609.

Chart 2

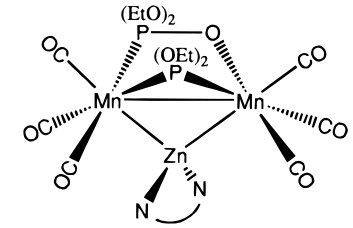

2

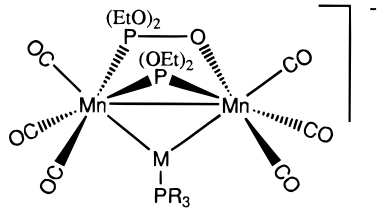

	M	R
3a	Au	Ph
3b	Au	Et
4	Ag	Ph
5a	Cu	Ph
5b	Cu	Et

it is clear that removal of two electrons from **1** takes place eventually in the HgI_2 reactions. Whether the deep green solution formed at low temperature contains a genuine manganese mercury cluster (which experiences an internal electron transfer process at higher temperatures), however, must be considered just as a possibility at present.

In contrast with the limited usefulness of anion **1** in the synthesis of manganese−group 12 metal clusters, the reactions of **1** with group 11 metal chloro complexes allow the synthesis of different heterometallic clusters in high yield. Thus, **1** reacts readily in tetrahydrofuran with 1 equiv of $[MCl(PR_3)]_n$ at room temperature to give the sodium salts of the corresponding anionic trinuclear clusters $[Mn_2M\{\mu\text{-}P(OEt)_2\}\{\mu\text{-}\eta^2\text{-}OP(OEt)_2\}(CO)_6(PR_3)]^-$ (**3**−**5**: **3a**, M = Au, R = Ph; **3b**, M = Au, R = Et; **4**, M = Ag, R = Ph; **5a**, M = Cu, R = Ph; **5b**, M = Cu, R = Et). These anionic clusters can be conveniently isolated as thermally stable orange solids after cation exchange of the sodium salts with $[AsPh_4]Cl$ in dichloromethane. The IR spectra of compounds **3**−**5** (Table 1) exhibit a pattern in the C−O stretching region very similar to that of complex **2**, and therefore a similar structure is assumed for these anions (Chart 2) As expected, the C−O stretching frequencies have values intermediate between those of the neutral **2** and dianion **1**.

Comparison between the IR or ^{31}P NMR spectra of the Na^+ and $[AsPh_4]^+$ salts of several of these anions (**3a** and **5a**; see Tables 1 and 2) reveals significant differences which must be taken as evidence for the presence of moderate ion-pairing effects.[13] Thus, the sodium salts exhibit higher ν_{st}(CO) frequencies than the corresponding tetraphenylarsonium salts, while none of the bands are significantly shifted toward lower wavenumbers. This is indicative of the absence of definite Mn−C−O···Na interactions.[13] Alternatively, we can envisage at least two types of interactions of the Na^+ cation that would be expected to yield a generalized

(13) Darensbourg, M. Y. *Prog. Inorg. Chem.* **1985**, *33*, 221.

Table 3. $^{31}P\{^1H\}$ NMR Data for New Compounds[a]

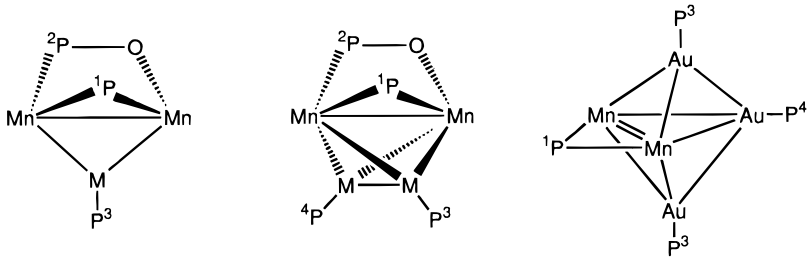

	δ/ppm				$J_{P,P}$/Hz					
compd	P^1	P^2	P^3	P^4	$J_{1,2}$	$J_{1,3}$	$J_{1,4}$	$J_{2,3}$	$J_{2,4}$	$J_{3,4}$
1[b,c]	419.3 (d)	153.2 (d)			60					
2	389.2 (br)	139.3 (br)								
3a (Na^+ salt)[c]	425.7 (d)	153.5 (vbr)	60.0 (br)		56					
3a	415.1 (d)	147.0 (br)	60.0 (d)		45			25		
3b	416.3 (br)	146.8 (br)	62.8 (d)					23		
4[d]	410.5 (d)	142.3 (br)	5.4 (2 × dd)[e]		51			13		
5a (Na^+ salt)[c]	415.3 (br)	147.8 (br)	−6.6 (br)							
5a	404.9 (br)	139.9 (br)	−8.3 (br)							
5b	406.3 (d, br)	140.7 (br)	−14.5 (br)		40					
6[f,g]	389.2 (ddd)	145.3 (ddd)	50.9 (ddd)[h]	49.4 (ddd)[h]	54	18	27	8	8	23
7[f]	388.9 (dd, br)	137.8 (d)	7.8 (2 × dd, br)[h,i]	6.2 (2 × ddd)[h,j]	46		30			10
8a[k]	410.0 (dt)		59.5 (dd)	44.7 (dt)		25	25			12
8b[k]	413.3 (dt)		65.7 (dd)	43.0 (dt)		24	24			12

[a] Recorded at 121.5 MHz in CD_2Cl_2 solution at room temperature, unless otherwise stated. Phosphorus atoms are labeled (P^1−P^4) according to the figures shown. [b] Data taken from ref 2. [c] In tetrahydrofuran/C_6D_6 solution (9:1), at room temperature. [d] Measured at 263 K. [e] $J(^{109}Ag-P) = 374$ Hz; $J(^{107}Ag-P) = 324$ Hz. [f] Measured at 203 K. [g] When measured at 293 K: δ 387.7 (d, $J_{1,2} = 57$, P^1), 145.2 (d, $J_{1,2} = 57$, P^2), 51.0 (br, P^3 and P^4). [h] Tentative assignment (see text). [i] $J(^{109}Ag-P) = 480$ Hz; $J(^{107}Ag-P) = 420$ Hz. [j] $J(^{109}Ag-P) = 440$ Hz; $J(^{107}Ag-P) = 390$ Hz. [k] C_6D_6 solution.

increase of the C−O stretching frequencies (a) with the oxygen-donor atom of the phosphonate group and (b) with the manganese atoms. The latter interaction should yield a higher increase in the ν(CO) bands than the former, as it reduces the negative charge at the dimanganese center in a stronger way. We then believe that interaction a is dominant in the case of anions **3**−**5**, as the measured shifts are moderate. However, we note that there is no clear correlation between the reduction of negative charge in the molecule (as deduced from IR data) and the ^{31}P chemical shifts of the phosphido and phosphonate groups (see Table 3). This possibly means that the real situation can not be adequately described by using a single type of cation−anion interaction for these trinuclear clusters.

Tetranuclear Derivatives. The trinuclear anions **3**−**5** (as their Na^+ salts) do not react with a second equivalent of the corresponding $[MCl(PR_3)]_n$ complexes in tetrahydrofuran at room temperature. They do react easily, however, in toluene solution, whereby neutral derivatives are obtained. In the case of the copper anion **5a**, electron transfer occurs, yielding $[Mn_2\{\mu\text{-P(OEt)}_2\}\{\mu\text{-}\eta^2\text{-OP(OEt)}_2\}(CO)_7(PPh_3)]$[2] as the major carbonyl-containing product. On the other hand, the silver and gold anions **4** and **3a** give the corresponding tetranuclear neutral clusters $[Mn_2M_2\{\mu\text{-P(OEt)}_2\}\{\mu\text{-}\eta^2\text{-OP(OEt)}_2\}(CO)_6(PPh_3)_2]$ (**6**, M = Au; **7**, M = Ag) in high yields.

Compounds **6** and **7** can be isolated as thermally stable red solids. However, they decompose slowly in solution, even at −20 °C. Thus, although spectroscopic characterization of these complexes in solution poses no special problems, all attempts to obtain single crystals for crystallographic studies were unsuccessful due to decomposition of the samples. In fact, the solution IR and ^{31}P NMR spectra of compounds **6** and **7** always showed the presence of small amounts of the anionic precursors **3a** and **4** (the effect is more pronounced for the silver compound). Thus, it seems that dissociation of a $[M(PPh_3)_3]^+$ unit from **6** and **7** is an easy process even in such weak donor solvents (S) as dichloromethane and toluene (eq 1).

$$\text{“}Mn_2\{\mu\text{-}M(PPh_3)\}_2\text{”} + xS \rightarrow \text{“}[Mn_2\{\mu\text{-}M(PPh_3)\}]^-\text{”} + \text{“}[MS_x(PPh_3)]^+\text{”} \quad (1)$$

This sort of decoordination process of $[M(PPh_3)]^+$ units has been observed previously in several heterometallic group 11 metal clusters upon addition of phosphines.[1d,f,8a,14]

The IR spectra of clusters **6** and **7** in the C−O stretching region are very similar to that of the zinc cluster **2** (Table 1), and therefore, a similar structure is proposed by replacing the (bipyridine)zinc fragment in **2** with a $M_2(PPh_3)_2$ moiety. We assume a tetrahedral geometry for the resulting tetrametallic Mn_2M_2 metal core (Chart 3). This requires the presence of a bonding interaction between the silver or gold atoms in these clusters. The latter is supported by the observation of coupling between the P atoms of the corresponding phosphine ligands (23 Hz for **6** and 10 Hz for **7**) in the range observed for the pentanuclear clusters **8a**,**b** (12 Hz), where Au−Au interactions have been confirmed through an X-ray study (see later). We note, however, that we have not been able to assign unambiguously the M−PPh_3 resonances in the spectra of complexes **6** and **7**, so that the chemical shifts assigned to P^3 could correspond to those of P^4 and *vice versa* (see Table 3).

(14) Evans, J.; Stroud, P. M. *J. Chem. Soc., Dalton Trans.* **1991**, 1351 and references therein.

Chart 3

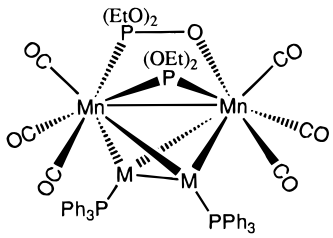

6 M = Au

7 M = Ag

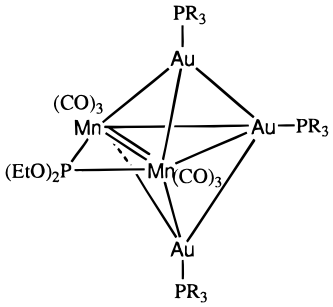

8a R =Ph

8b R = Et

This, of course, does not introduce uncertainty about the value of the mutual coupling in these resonances.

Further confirmation of the structure of clusters **6** and **7** comes from comparison with the isoelectronic rhenium− or manganese−gold clusters $[M_2(AuPPh_3)_2\{\mu\text{-}C(O)R'\}(\mu\text{-}PR_2)(CO)_6]$ (M = Re, R = Ph, R′ = Me, Bu, Ph;[15] M = Mn, R = Ph, Cy, R′ = Me, Ph[9]), for which tetrahedral metal cores have been found crystallography. Indeed, spectroscopic data (ν(CO) and ^{31}P NMR) for these acyl-containing clusters are very similar to those of **6** and **7**. Although P−P couplings were not measured for the manganese clusters,[9] the rhenium species showed ^{31}P−^{31}P couplings between Au−PPh$_3$ moieties of *ca*. 25 Hz,[15] very close to that observed for **6**.

In contrast with the above-mentioned acyl clusters, which appear to be rigid in solution, cluster **6** exhibits dynamic behavior. Thus, although the low-temperature ^{31}P NMR spectrum of **6** shows two distinct chemical environments for the AuPPh$_3$ groups of the cluster, in agreement with the proposed structure, an averaged spectrum is observed at room temperature (Table 3). The process does not much affect the other phosphorus-containing group of the molecule, as judged from chemical shifts and couplings. To explain these observations, we propose a fluxional process involving the metal core, as shown in Figure 2. The rearrangement requires the cleavage of two Mn−Au bonds to yield a transient structure with a square-planar Mn_2Au_2 skeleton, which reverts again to the tetrahedral geometry. This should not require much energy, given the fact that complex **6** dissociates a $[MPPh_3]^+$ unit easily in solution (*i.e.* the Mn−Au bonds are not very strong; see eq 1). In fact, coalescence of the separated resonances corresponding to the AuPh$_3$ moieties in **6** occurs at *ca* 250 K, which yields an estimated value[16] for the corresponding activation barrier ($\Delta G^{\ddagger}$) of *ca*. 48 kJ mol^{-1}, a fairly low figure. On the other hand, the proposal of a transient square-planar skeleton is not unreasonable, as some stable clusters with that metal core geometry are known (for example, the clusters $[Fe_2Au_2(CO)_8\{\mu\text{-}Ph_2P(CH_2)_nPPh_2\}]$ (n = 1−3).[17] Furthermore, we note that related metal core rearrangements have been proposed to explain the solution dynamics of several ruthenium−group 11 clusters.[18] Finally, it is quite likely that the silver cluster **7** experiences a dynamic process similar to that just shown for **6**. However, experimental confirmation for this was not possible, due to relatively rapid thermal decomposition of the samples at room temperature, added to the occurrence of Ag−P bond dissociation at these temperatures, something commonly observed for phosphine ligands coordinated to silver(I) atoms.[19]

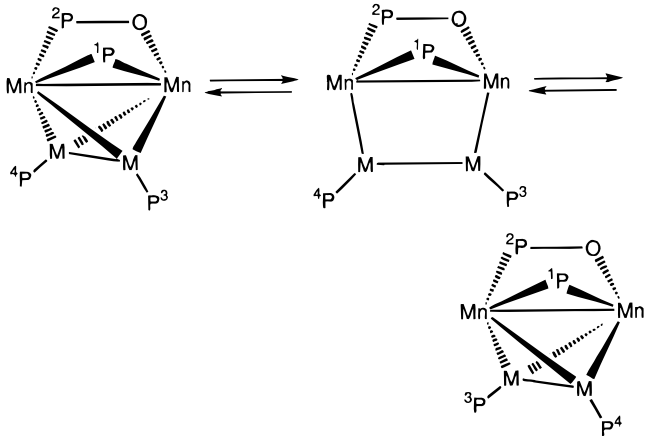

Figure 2. Schematic view of the fluxional rearrangement proposed for compound **6** in solution (P^1 or P^2 = P(OEt)$_2$; P^3 or P^4 = PPh$_3$; Mn = Mn(CO)$_3$).

Pentanuclear Derivatives. As we have stated before, the tetranuclear clusters **6** and **7** decompose slowly in solution. During our attempts to obtain single crystals of the gold cluster **6**, we noted the presence of very small amounts of a blue neutral species, which we have characterized as the pentanuclear unsaturated cluster $[Mn_2Au_3\{\mu\text{-}P(OEt)_2\}(CO)_6(PPh_3)_3]$ (**8a**; Chart 3). Further experiments have shown that yields of **8a** can be increased when a toluene solution of **6** is mixed with 1 equiv of [AuCl(PPh$_3$)] (or **3a** with 2 equiv of the gold complex, in toluene) and exposed to UV light or placed in contact with aluminum oxide. A related PEt$_3$ derivative, **8b**, can be obtained analogously from **3b** and 2 equiv of [AuCl(PEt$_3$)]. In neither case, however, have we found conditions to increase the yields above *ca*. 15%.

The structure of the pentanuclear clusters **8** has been confirmed through an X-ray study on the triphenylphosphine derivative **8a**. The structure of **8a** is shown in Figure 3 together with the atom-numbering scheme. Selected bond distances and angles are given in Table 4.

(15) Haupt, H. J.; Heinekamp, C.; Flörke, U. *Inorg. Chem.* **1990**, *29*, 2955.

(16) Calculated using the modified Eyring equation $\Delta G^{\ddagger} = 19.14T_c[9.97 + \log(T_c/\Delta\nu)]$ (J mol^{-1}). See: Günter, H. *NMR Spectroscopy*; Wiley; New York, 1980; p 243.

(17) Alvarez, S.; Rossell, O.; Seco, M.; Valls, J.; Pellinghelli, M. A.; Tiripicchio, A. *Organometallics* **1991**, *10*, 2309.

(18) Orpen, A. G.; Salter, I. D. *Organometallics* **1991**, *10*, 111 and references therein.

(19) (a) Verkade, J. G.; Socol, S. M. *Inorg. Chem.* **1984**, *23*, 3487. (b) Freeman, M. J.; Orpen, A. G.; Salter, I. D. *J. Chem. Soc., Dalton Trans.* **1987**, 379.

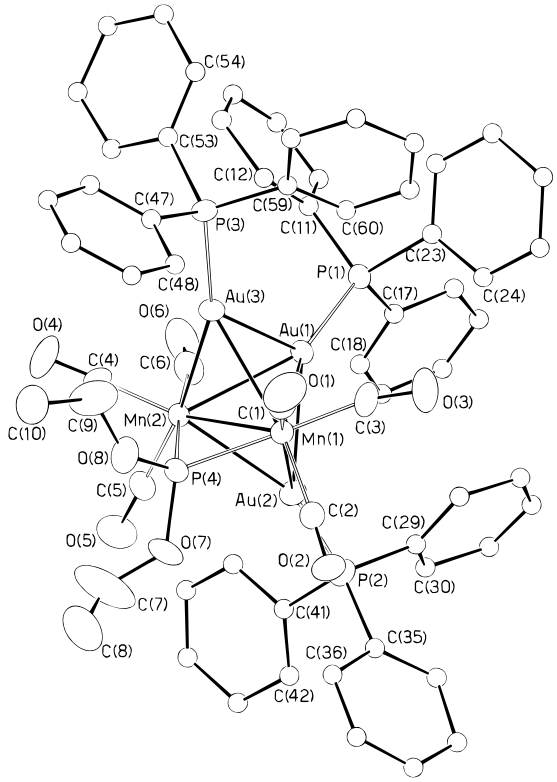

Figure 3. Molecular structure of **8a**, with the atom-numbering scheme.

Table 4. Selected Bond Distances (Å) and Angles (deg) in Complex 8a

Au(1)−Au(2)	2.797(1)	Au(3)−P(3)	2.312(4)
Au(1)−Au(3)	2.771(1)	Mn(1)−Mn(2)	2.749(3)
Au(1)−Mn(1)	2.701(2)	Mn(1)−P(4)	2.193(4)
Au(1)−Mn(2)	2.722(2)	Mn(2)−P(4)	2.189(4)
Au(1)−P(1)	2.292(4)	Mn(1)−C(1)	1.814(16)
Au(2)−Mn(1)	2.740(2)	Mn(1)−C(2)	1.795(16)
Au(2)−Mn(2)	2.764(2)	Mn(1)−C(3)	1.801(16)
Au(2)−P(2)	2.315(4)	Mn(2)−C(4)	1.764(15)
Au(3)−Mn(1)	2.778(3)	Mn(2)−C(5)	1.760(15)
Au(3)−Mn(2)	2.738(2)	Mn(2)−C(6)	1.828(17)
Au(3)−Au(1)−Mn(2)	59.8(1)	Au(3)−Mn(2)−Mn(1)	60.8(1)
Au(3)−Au(1)−Mn(1)	61.0(1)	Au(2)−Mn(2)−Mn(1)	59.6(1)
Au(2)−Au(1)−Mn(2)	60.1(1)	Au(2)−Mn(2)−Au(3)	111.4(1)
Au(2)−Au(1)−Mn(1)	59.7(1)	Au(2)−Mn(1)−Au(3)	111.0(1)
Au(2)−Au(1)−Au(3)	109.5(1)	Au(1)−Mn(1)−Au(3)	60.7(1)
Au(1)−Au(2)−Mn(2)	58.6(1)	Au(1)−Mn(1)−Au(2)	61.9(1)
Au(1)−Au(2)−Mn(1)	58.4(1)	Au(1)−Mn(1)−Mn(2)	59.9(1)
Au(1)−Au(3)−Mn(2)	59.2(1)	Au(1)−Mn(2)−Au(3)	61.0(1)
Au(1)−Au(3)−Mn(1)	58.3(1)	Au(1)−Mn(2)−Au(2)	61.3(1)
Mn(1)−Au(2)−Mn(2)	59.9(1)	Mn(1)−Mn(2)−C(6)	123.9(5)
Mn(1)−Au(3)−Mn(2)	59.8(1)	Mn(1)−Mn(2)−C(5)	120.6(5)
Mn(2)−Mn(1)−C(2)	121.5(5)	Mn(1)−Mn(2)−C(4)	129.8(5)
Mn(2)−Mn(1)−C(3)	123.7(5)	Mn(2)−Mn(1)−C(1)	127.6(5)
C(2)−Mn(1)−C(3)	92.8(7)	C(5)−Mn(2)−C(6)	92.9(7)
C(1)−Mn(1)−C(3)	90.2(7)	C(4)−Mn(2)−C(6)	89.0(7)
C(1)−Mn(1)−C(2)	91.2(6)	C(4)−Mn(2)−C(5)	90.2(7)
P(4)−Mn(1)−C(2)	89.6(5)	P(4)−Mn(2)−C(5)	90.0(5)
P(4)−Mn(1)−C(1)	94.6(5)	P(4)−Mn(2)−C(4)	95.0(5)
P(4)−Mn(1)−C(3)	174.6(5)	P(4)−Mn(2)−C(6)	175.0(5)
Mn(1)−C(1)−O(1)	175.8(14)	Mn(2)−C(4)−O(4)	176.2(13)
Mn(1)−C(2)−O(2)	176.1(14)	Mn(2)−C(5)−O(5)	178.2(14)
Mn(1)−C(3)−O(3)	161.2(14)	Mn(2)−C(6)−O(6)	167.0(15)
Mn(1)−P(4)−Mn(2)	77.7(1)		

The molecule displays a slightly distorted trigonal-bipyramidal Mn_2Au_3 metal core, with the manganese atoms at equatorial sites. The Mn atoms are symmetrically bridged by a diethoxyphosphido group (Mn(1)−P(4) = 2.193(4) Å and Mn(2)−P(4) = 2.189(4) Å). The coordination environment around each manganese atoms is completed by three carbonyl atoms. Two of the six carbonyls can be considered semibridging, as evidenced by the short Au···C separations (Au(1)−C(3) = 2.508(16) Å and Au(1)−C(6) = 2.555(16) Å) and by the values of the Mn−C−O angles (Mn(1)−C(3)−O(3) = 161.2(14)° and Mn(2)−C(6)−O(6) = 167.0(15)°). Even though the isolobal analogy H/AuPR$_3$[20] usually breaks down when more than one gold(I) phosphine unit is present in a cluster,[1d,f] is still useful in relating compounds **8** with the yet unknown trihydrides [$Mn_2(\mu$-H)$_3$(μ-PR$_2$)(CO)$_6$]. We note, however, that a deprotonated derivative of the latter, namely [$Mn_2(\mu$-H)$_2$(μ-PPh$_2$)(CO)$_6$]$^-$, has been reported.[21] Consideration of the effective atomic number rule leads us to propose a formal double bond between manganese atoms for all these species. Although this is a localized-bond view of the electronic structure of the clusters **8**, it is in agreement with the experimental Mn−Mn distance found for **8a**, 2.749(3) Å, which is very close to those found for the unsaturated dihydride [$Mn_2(\mu$-H)$_2$(CO)$_6$(μ-Ph$_2$PCH$_2$PPh$_2$)] (2.699(2) Å)[22] or for the also unsaturated cluster [$Mn_2(\mu$-H)(μ-AuPPh$_3$)(CO)$_6${μ-(EtO)$_2$POP(OEt)$_2$}] (2.739(3) Å).[6] We then conclude that the electron deficiency of clusters **8** is mainly localized between the manganese atoms. This fact is probably responsible for the short Mn−P distances in the bridging phosphido ligand, which are *ca*. 0.03 Å shorter than those found in the electron-precise cluster **2** and *ca*. 0.1 Å shorter than those in the complexes [Mn_2{μ-P(OEt)$_2$}{μ-η^2-OP(OEt)$_2$}(CO)$_x$L] (L = PPh$_3$, x = 7; L = Me$_2$PCH$_2$PMe$_2$, x = 6),[2] where no Mn−Mn bond is present.

The structure of **8a** is very similar to those previously established for the isoelectronic clusters [$M_2Au_3(\mu$-PPh$_2$)(CO)$_6$(PPh$_3$)$_3$] (M = Mn,[9] Re[15]), which are obtained in low yields from the reaction of the corresponding complexes [$M_2(\mu$-H)(μ-PPh$_2$)(CO)$_8$] with RLi followed by addition of [AuCl(PPh$_3$)]. As shown in Table 5, the average intermetallic distances are very similar, after allowing for the larger covalent radius of rhenium, if necessary. In particular, the Au−Au lengths for the manganese clusters fall in the lower part of the range found for heterometallic clusters containing gold(I) bonding interactions (usually in the range 2.70−3.10 Å)[1f] and are significantly shorter than those in metallic gold (2.884 Å).[23] This is perhaps another consequence of the electronic deficiency of these compounds. In contrast, the Mn−Au distances are not particularly short, as can be seen by comparison with the intermetallic distances in the cluster [$MnAu_4$(CO)$_4$(PPh$_3$)$_4$]BF$_4$,[24] which can be classified as an electron-precise cluster. We have encountered this effect previously.[6]

The pathway through which clusters **8** are formed from **6** remains unknown to us. Particularly intriguing is the way in which the robust phosphonate ligand present in **6** is lost during the reaction. As we have

(20) Evans, D. G.; Mingos, D. M. P. *J. Organomet. Chem.* **1982**, *232*, 171.
(21) (a) Henrick, K.; Iggo, J. A.; Mays, M J.; Raithby, P. R. *J. Chem. Soc., Chem. Commun.* **1984**, 209. (b) Henrick, K.; McPartlin, M.; Iggo, J. A.; Kemball, A. C.; Mays, M. J.; Raithby, P. R. *J. Chem. Soc., Dalton Trans.* **1987**, 2669.
(22) García Alonso, F. J.; García Sanz, M.; Riera, V.; Ruiz, M. A.; Tiripicchio, A.; Tiripicchio-Camellini, M. *Angew. Chem., Int. Ed. Engl.* **1988**, *27*, 1167.
(23) Pearson, W. B. *Lattice Spacings and Structures of Metals and Alloys*; Pergamon: Oxford, U.K., 1957.
(24) Nicholson, B. K.; Bruce, M. I.; bin Shawkataly, O.; Tiekink, E. R. T. *J. Organomet. Chem.* **1992**, *440*, 411.

Table 5. Selected Intermetallic Distances in Group 7 Metal−Gold Clusters with Trigonal-Bipyramidal Core Geometry[a]

compd	M−M	M−Au$_e$	M−Au$_a$	Au$_a$−Au$_e$	Au$_e$−Au$_e$	ref
8a	2.749(3)	2.712(2)	2.755(2)	2.784(1)		this work
$[Mn_2(\mu\text{-}PPh_2)(CO)_6(AuPPh_3)_3]$	2.747(4)	2.716(2)	2.740(2)	2.798(1)		9
$[Re_2(\mu\text{-}PPh_2)(CO)_6(AuPPh_3)_3]$	2.914(3)	2.816(3)	2.838(3)	2.829(3)		15
$[Mn(CO)_4(AuPPh_3)_4]BF_4$		2.761(4)	2.655(4)	2.874(2)	2.789(2)	24

[a] The subscripts a and e refer to the axial and equatorial positions of the trigonal bipyramid, respectively. When more than one value for a given type of intermetallic distance is present, an average figure is given.

noted above, we have not been able to find conditions to obtain compounds **8** in yields higher than 15%; thus, we have not tried to follow the fate of that ligand. Attempts to identify the driving force for the extrusion of the phosphonate group were unsuccessful. For example, treatment of **6** with [AuMe(PPh$_3$)] (so as to form **8a** and P(OEt)$_2$(OMe)) gave extremely poor yields of **8a**. Although in the end we cannot propose an explanation for the formation of clusters **8**, we note that the above-mentioned related clusters $[M_2Au_3(\mu\text{-}PPh_2)(CO)_6(PPh_3)_3]$ are formed from a tetranuclear precursor through the extrusion of a bridging acyl ligand, which is isoelectronic with the phosphonate group. In that case, however, it was found[9,15] that the tetranuclear clusters related to **6** were not precursors for the pentanuclear compounds. Therefore, it seems that the extrusion of the acyl group follows from a pathway different from that operating in our system.

Comment on the ^{31}P Chemical Shifts of the Diethoxyphosphido Bridging Group. ^{31}P NMR spectroscopy is a particularly useful tool for the structural study of the vast family of organometallic compounds which contain bridging phosphido ligands. Analysis of the experimental data for a large number of this sort of complex indicates that the presence of bonding interactions between atoms bridged by phosphido ligands causes a strong deshileding of the corresponding ^{31}P resonances, although exceptions to this effect are known.[25] Inspection of Table 2 reveals that, for the compounds described in this work (all of which are metal−metal-bonded species), the diethoxyphosphido resonance falls in the range *ca.* 425−380 ppm. On the other hand, this range is *ca.* 373−345 ppm for nine derivatives of anion **2** obtained through oxidation reactions, all of which lack a manganese−manganese bond.[2] Therefore, we conclude that the presence of a metal−metal bond in these dimanganese complexes bridged by diethoxyphosphido and diethylphosphonate groups induces only a moderate deshielding on the ^{31}P resonances of the phosphido ligand, so that the latter cannot be used as a reliable probe for the metal−metal interaction. Incidentally, the effect of the metal−metal bond on the chemical shift of the phosphonate resonance is just the opposite; that is, the non-metal−metal-bonded species display higher chemical shifts (in the range *ca.* 170−180 ppm)[2] than the metal−metal-bonded compounds described in this work (in the range 138−153 ppm).

In a study on a series of metal−metal-bonded diiron compounds bridged by alkoxyphosphido and related ligands, it was found that the ^{31}P chemical shift varies linearly with the CO stretching frequencies of the complexes (the latter being taken as an indicator of the charge at the P atoms). In contrast with this, the ^{31}P chemical shifts of the phosphido group in compounds **1**−**8** show the opposite general trend, so that the neutral derivatives display lower chemical shifts than the anionic ones. Besides, we note that there is no correlation between ν_{st}(CO) frequencies and ^{31}P shifts in our compounds, even within the isostructural group of clusters **3**−**5**. This is not completely unreasonable, as it is known that an increase of the positive charge at an atom can induce either an increase or a decrease in the paramagnetic contribution to the chemical shielding of the nucleus (σ_p), depending on which of the factors influencing σ_p (HOMO−LUMO gap, orbital contribution, etc.)[26] prevails. In addition, other factors, such as the magnetic anisotropy of the different groups in these molecules, may be of relevance when comparing two otherwise quite similar structures (*e.g.* PPh$_3$ and PEt$_3$ derivatives).

Experimental Section

General Considerations. All manipulations and reactions were carried out under a nitrogen atmosphere using standard Schlenk techniques. Solvents were purified according to standard literature procedures[27] and distilled under nitrogen prior to use. Petroleum ether refers to that fraction distilling in the range 60−65 °C. Tetrahydrofuran solutions of compound **1**[2] and the complexes [AuCl(PR$_3$)],[28] [CuCl(PR$_3$)]$_4$ (R = Ph, Et),[29] [AgCl(PPh$_3$)]$_4$,[30] and [ZnCl$_2$(bpy)][31] were prepared according to literature procedures. In the case of compound **1** a 100% yield in its formation was assumed.[2] All other reagents were purchased from the usual commercial suppliers and used as received. Filtrations were carried out using diatomaceous earth. Alumina for column chromatography was deactivated by appropriate addition of water to the commercial material (Aldrich, neutral activity I). Tap-water-cooled jacketed columns were used for this purpose. NMR spectra were measured at 300.13 MHz (^{1}H) and 121.50 MHz (^{31}P, proton decoupled). Chemical shifts (δ) are given in ppm, relative to internal TMS (^{1}H) or external 85% H$_3$PO$_4$ aqueous solution (^{31}P), with positive values for frequencies higher than that of the reference. Coupling constants (J) are given in hertz.

Preparation of $[Mn_2Zn\{\mu\text{-}P(OEt)_2\}\{\mu\text{-}\eta^2\text{-}OP(OEt)_2\}(CO)_6(bpy)]$ (2). A tetrahydrofuran solution (15 mL) containing 0.076 mmol of anion **1** was added into a Schlenk flask containing 0.022 g of [ZnCl$_2$(bpy)] (0.076 mmol) cooled to −80 °C. The mixture was then stirred and allowed to reach room temperature over 1 h and then further stirred at that temperature for 0.5 h, to give a red solution. Solvent was then removed under vacuum and the residue extracted with diethyl

(25) Carty, A. J.; MacLaughin, S. A.; Nucciarone, D. In *Phosphorus-31 NMR Spectroscopy in Stereochemical Analysis*; Verkade, J. G., Quin, L. D., Eds.; VCH: New York, 1987; Chapter 13.

(26) Jameson, C. J.; Mason, J. In *Multinuclear NMR*; Mason, J., Ed.; Plenum Press: New York, 1987; Chapter 3.

(27) Perrin, D. D.; Armarego, W. L. F. *Purification of Laboratory Chemicals*; Pergamon Press: Oxford, U.K., 1988.

(28) Braunstein, P.; Lehner, H.; Matt, D. *Inorg. Synth.* **1990**, *27*, 218.

(29) Cariati, F.; Naldini, L. *Gazz. Chim. Ital.* **1965**, *95*, 3.

(30) Cariati, F.; Naldini, L. *Gazz. Chim. Ital.* **1965**, *95*, 201.

(31) Postmus, C.; Ferraro, J. R.; Wozniak, W. *Inorg. Chem.* **1967**, *6*, 2030.

Table 6. Experimental Data for the X-ray Diffraction Studies

	2	**8a**
mol formula	$C_{24}H_{28}Mn_2N_2O_{11}P_2Zn$	$C_{64}H_{55}Au_3Mn_2O_8P_4$
mol wt	757.70	1776.80
cryst syst	monoclinic	monoclinic
space group	$P2_1/c$	$P2_1/c$
radiatn	niobium-filtered Mo Kα (λ = 0.710 73 Å)	graphite-monochromated Mo Kα (λ = 0.710 73 Å)
a, Å	16.776(6)	21.829(6)
b, Å	17.948(6)	13.434(5)
c, Å	10.753(4)	21.063(6)
β, deg	102.53(2)	93.01(1)
V, Å^3	3161(2)	6168(3)
Z	4	4
D_{calcd}, g cm^{-3}	1.592	1.913
F(000)	1536	3400
cryst dimens, mm	0.13 × 0.18 × 0.22	0.22 × 0.25 × 0.35
μ(Mo Kα), cm^{-1}	16.97	76.66
2θ range, deg	6−48	6−48
rflns measd	±h,k,l	±h,k,l
no. of unique total data	4974	10358
no. of unique obsd data	1443 ($I > 2\sigma(I)$)	5014 ($I > 2\sigma(I)$)
R^a	0.0535	0.0377
$R_w{}^b$	0.0466	0.0388

[a] $R = \sum||F_o| - |F_c||/\sum|F_o|$. [b] $R_w = [\sum_w(|F_o| - |F_c|)^2/\sum_w(F_o)^2]^{1/2}$.

ether (2 × 10 mL) and filtered. Crystallization of the filtrate from diethyl ether/petroleum ether at −20 °C gave red crystals of complex **2** (0.041 g, 70%). The crystals used in the X-ray study were grown from a dichloromethane/petroleum ether solution of **2** at −20 °C. Anal. Calcd for $C_{24}H_{28}Mn_2N_2O_{11}P_2Zn$: C, 38.04; H, 3.73; N, 3.70. Found: C, 37.56; H, 3.81; N, 3.52. ^{1}H NMR (CD_2Cl_2): δ 9.60, 8.52, 8.21, 7.86, 7.66 (5 × m, 5 × 1H, bpy), 8.40−8.30 (m, 3H, bpy), 4.47−4.33 (m, 4H, OCH_2), 3.75−3.60 (m, 4H, OCH_2), 1.46, 1.44, 1.24, 1.12 (4 × t, J_{HH} = 7, 12H, Me).

Preparation of [AsPh$_4$][Mn$_2$Au{μ-P(OEt)$_2$}{μ-η^2-OP(OEt)$_2$}(CO)$_6$(PPh$_3$)] (3a). A tetrahydrofuran solution (10 mL) containing 0.1 mmol of **1** was added into a Schlenk flask containing [AuCl(PPh$_3$)] (0.05 g, 0.1 mmol) at −20 °C, and the mixture was stirred for 15 min to yield a solution of **3a** as its Na^+ salt, as revealed by IR and ^{31}P NMR spectroscopy. The solvent was then removed under vacuum and the residue dissolved in dichloromethane (10 mL) and stirred with [AsPh$_4$]Cl (0.042 g, 0.1 mmol) for 10 min to give an orange solution, which was filtered. Solvent was then removed under vacuum and the residue dissolved again in tetrahydrofuran and filtered to ensure removal of any residual [AsPh$_4$]Cl. Evaporation of solvent from the filtrate and washing of the residue with petroleum ether (3 × 5 mL) gave compound **3a** as an orange powder (0.124 g, 90%). Crystallization of the latter from a dichloromethane/petroleum ether solution at −20 °C yielded red-orange crystals of **3a** which were unsuitable for single-crystal X-ray studies. Anal. Calcd for $C_{56}H_{55}AsAuMn_2O_{11}P_3$: C, 48.79; H, 4.02. Found: C, 48.37; H, 4.02. ^{1}H NMR (CD_2Cl_2): δ 7.79−7.25 (m, 35H, Ph), 4.28−4.08 (complex, 4H, OCH_2), 3.64−3.31 (complex, 4H, OCH_2), 1.27, 1.20, 0.91, 0.83 (4 × t, J_{HH} = 7, 12H, Me).

Preparation of [AsPh$_4$][Mn$_2$Au{μ-P(OEt)$_2$}{μ-η^2-OP(OEt)$_2$}(CO)$_6$(PEt$_3$)] (3b). By the procedure described for **3a**, but using [AuCl(PEt$_3$)] (0.035 g, 0.1 mmol) instead, compound **3b** was isolated as an orange solid (0.105 g, 85%). Crystallization of the latter from a dichloromethane/petroleum ether solution at −20 °C yields red-orange crystals of **3b**. Anal. Calcd for $C_{44}H_{55}AsAuMn_2O_{11}P_3$: C, 42.80; H, 4.50. Found: C, 42.84; H, 4.34. ^{1}H NMR (CD_2Cl_2): δ 7.80−7.30 (m, 20H, Ph), 4.30−4.10 (complex, 4H, OCH_2), 3.75 (m, 1H, OCH_2), 3.50−3.40 (complex, 3H, OCH_2), 1.82 (qn, $J_{HH} = J_{PH}$ = 8, 6H, PCH_2), 1.17 (dt, J_{PH} = 18, J_{HH} = 8, 9H, PCH_2CH_3), 1.27, 1.21, 1.00, 0.92 (4 × t, J_{HH} = 7, 12H, OCH_2CH_3).

Preparation of [AsPh$_4$][Mn$_2$Ag{μ-P(OEt)$_2$}{μ-η^2-OP(OEt)$_2$}(CO)$_6$(PPh$_3$)] (4). By the procedure described for **3a**, but using [AgCl(PPh$_3$)]$_4$ (0.041 g, 0.1 mequiv) instead, compound **4** was isolated as an orange solid (0.114 g, 89%). Crystallization of the latter from a dichloromethane/petroleum ether solution at −20 °C yields red-orange crystals of **4**. Anal. Calcd for $C_{56}H_{55}AgAsMn_2O_{11}P_3$: C, 52.16; H, 4.30. Found: C, 52.25; H, 4.35. ^{1}H NMR (CD_2Cl_2, 263 K): δ 7.88−7.42 (m, 35H, Ph), 4.34−4.13 (complex, 4H, OCH_2), 3.65−3.40 (complex, 4H, OCH_2), 1.33, 1.31, 1.01, 0.98 (4 × t, J_{HH} = 7, 12H, Me).

Table 7. Atomic Coordinates (×10^4) and Equivalent Isotropic Thermal Parameters (Å^2 × 10^4) for the Non-Hydrogen Atoms of Complex 2

atom	x	y	z	$U_{eq}{}^a$
Zn	1219(1)	451(1)	2375(2)	607(12)
Mn(1)	2038(2)	244(2)	778(3)	565(16)
Mn(2)	2646(2)	963(2)	3231(3)	680(17)
P(1)	3214(4)	116(4)	2192(6)	769(33)
P(2)	2376(4)	1442(4)	721(7)	689(32)
O(1)	1641(10)	−1330(8)	1088(16)	957(86)
O(2)	386(9)	616(11)	−663(13)	1000(87)
O(3)	2731(10)	−162(11)	−1401(15)	1409(103)
O(4)	2441(10)	−118(11)	5125(14)	1125(97)
O(5)	1623(12)	2131(11)	3995(21)	1698(127)
O(6)	4065(11)	1467(12)	5009(17)	1392(110)
O(7)	2915(8)	1726(8)	1931(15)	939(81)
O(8)	2880(11)	1733(10)	−353(19)	1316(112)
O(9)	1582(8)	1975(8)	379(13)	833(75)
O(10)	3368(10)	−722(9)	2750(15)	1136(96)
O(11)	4064(10)	262(12)	1674(17)	1540(112)
N(1)	618(12)	−342(10)	3236(16)	646(89)
N(2)	126(9)	1003(13)	2331(16)	659(91)
C(1)	1785(14)	−682(13)	998(23)	694(119)
C(2)	1024(13)	497(13)	−68(17)	667(103)
C(3)	2466(12)	−16(12)	−518(22)	682(115)
C(4)	2478(14)	333(17)	4341(23)	922(138)
C(5)	2013(14)	1662(13)	3641(23)	940(137)
C(6)	3478(17)	1269(15)	4278(24)	1002(150)
C(7)	2598(29)	1712(22)	−1497(40)	2342(219)
C(8)	3306(17)	1710(15)	−2133(25)	1512(115)
C(9)	1658(15)	2804(15)	357(23)	1077(91)
C(10)	906(19)	3078(15)	−450(27)	1679(119)
C(11)	4031(16)	−858(16)	3738(26)	1220(105)
C(12)	3780(15)	−1564(15)	4292(22)	1295(98)
C(13)	4614(28)	710(23)	2201(38)	2371(216)
(C14)	5405(21)	402(19)	2014(30)	2251(155)
C(15)	868(14)	−1040(18)	3507(21)	824(130)
C(16)	367(23)	−1610(15)	3912(23)	1099(159)
C(17)	−449(21)	−1363(22)	3970(27)	1193(182)
C(18)	−673(17)	−630(17)	3654(24)	883(140)
C(19)	−183(14)	−92(18)	3282(19)	686(120)
C(20)	−413(16)	652(14)	2869(24)	647(128)
C(21)	−1144(14)	964(18)	2987(20)	761(125)
C(22)	−1321(18)	1686(18)	2577(26)	1022(154)
C(23)	−790(15)	2077(15)	2033(24)	937(142)
C(24)	−58(16)	1690(13)	1947(21)	752(125)

[a] Defined as one-third of the trace of the orthogonalized $\mathbf{U}_{ij}$ tensor.

Preparation of [AsPh$_4$][Mn$_2$Cu{μ-P(OEt)$_2$}{μ-η^2-OP(OEt)$_2$}(CO)$_6$(PPh$_3$)] (5a). By the procedure described for **3a**, but using [CuCl(PPh$_3$)]$_4$ (0.036 g, 0.1 mequiv) and a reaction time of 30 min instead, compound **5a** was isolated as an orange solid (0.105 g, 84%). Crystallization of the latter from a dichloromethane/diethyl ether solution at −20 °C yields red-orange crystals of **5a**. Anal. Calcd for $C_{56}H_{55}AsCuMn_2O_{11}P_3$: C, 54.01; H, 4.46. Found: C, 54.43; H, 4.56. ^{1}H NMR (CD_2Cl_2): δ 7.75−7.33 (m, 35H, Ph), 4.26−4.13 (complex, 4H, OCH_2), 3.56−3.50 (complex, 4H, OCH_2), 1.29 (t, J_{HH} = 7, 6H, Me), 1.05, 1.01 (2 × t, J_{HH} = 7, 6H, Me).

Preparation of [AsPh$_4$][Mn$_2$Cu{μ-P(OEt)$_2$}{μ-η^2-OP(OEt)$_2$}(CO)$_6$(PEt$_3$)] (5b). By the procedure described for **3a**, but using [CuCl(PEt$_3$)]$_4$ (0.022 g, 0.1 mequiv) instead, compound **5b** was isolated as an orange solid (0.095 g, 85%). Crystallization of the latter from a dichloromethane/diethyl ether solution at −20 °C yields red-orange crystals of **5b**. Anal. Calcd for $C_{44}H_{55}AsCuMn_2O_{11}P_3$: C, 47.99; H, 5.03. Found: C, 47.47; H, 4.79. ^{1}H NMR (CD_2Cl_2): δ 7.79−7.19 (m, 20H, Ph),

Table 8. Atomic Coordinates (×10⁴) and Equivalent Isotropic Thermal Parameters (Å² × 10⁴) for the Non-Hydrogen Atoms of Complex 8a

atom	*x*	*y*	*z*	U_{eq}[a]	atom	*x*	*y*	*z*	U_{eq}[a]
Au(1)	2412.8(2)	−92.0(4)	2046.0(2)	375(2)	C(25)	3235(9)	770(15)	4316(10)	974(63)
Au(2)	1943.2(3)	1455.8(4)	1277.1(3)	471(2)	C(26)	3458(8)	−22(14)	4696(8)	775(53)
Au(3)	3269.9(3)	−1154.1(4)	1396.5(3)	407(2)	C(27)	3258(8)	−1021(13)	4590(8)	727(50)
Mn(1)	3149.6(9)	896.0(15)	1270.2(9)	356(7)	C(28)	2832(7)	−1206(11)	4077(7)	567(42)
Mn(2)	2255.6(9)	−358.1(15)	766.5(9)	357(7)	C(29)	931(7)	2874(11)	2175(7)	564(42)
P(1)	2079(2)	−620(3)	3003(2)	401(13)	C(30)	300(7)	3090(12)	2258(8)	702(49)
P(2)	1205(2)	2674(3)	1380(2)	449(14)	C(31)	135(9)	3324(14)	2904(9)	882(58)
P(3)	4024(2)	−2266(3)	1741(2)	407(13)	C(32)	580(10)	3262(15)	3377(10)	965(63)
P(4)	2960(2)	456(3)	277(2)	420(13)	C(33)	1152(10)	2966(15)	3314(10)	1004(67)
O(1)	4482(5)	728(9)	1225(7)	937(59)	C(34)	1360(8)	2745(14)	2687(9)	820(54)
O(2)	3247(5)	2958(8)	847(5)	636(44)	C(35)	1453(6)	3913(11)	1156(7)	475(38)
O(3)	3396(6)	1617(9)	2574(6)	937(57)	C(36)	1787(8)	3960(13)	599(8)	714(48)
O(4)	2336(6)	−2167(9)	29(6)	997(60)	C(37)	1942(8)	4950(14)	405(9)	880(58)
O(5)	1317(5)	348(10)	−170(6)	889(53)	C(38)	1795(8)	5761(14)	706(9)	831(55)
O(6)	1302(6)	−1451(11)	1426(5)	974(59)	C(39)	1475(8)	5735(13)	1258(8)	741(50)
O(7)	2769(5)	1325(8)	−224(5)	797(49)	C(40)	1306(7)	4746(11)	1502(7)	583(42)
O(8)	3468(5)	−40(8)	−149(5)	702(45)	C(41)	521(7)	2474(12)	866(7)	571(41)
C(1)	3974(7)	755(10)	1244(7)	498(57)	C(42)	190(8)	3253(13)	609(8)	727(51)
C(2)	3195(7)	2172(12)	1024(7)	490(57)	C(43)	−361(10)	3036(17)	177(10)	1031(68)
C(3)	3234(7)	1215(11)	2101(8)	600(62)	C(44)	−481(10)	2050(17)	71(10)	1039(68)
C(4)	2326(7)	−1462(10)	322(7)	491(55)	C(45)	−193(11)	1287(17)	375(11)	1213(79)
C(5)	1693(7)	82(11)	207(7)	545(58)	C(46)	376(9)	1484(15)	759(10)	957(62)
C(6)	1690(7)	−981(13)	1238(8)	637(67)	C(47)	4595(6)	−2469(11)	1152(6)	466(37)
C(7)	2577(16)	1205(27)	−855(13)	2092(192)	C(48)	4958(8)	−1638(12)	997(8)	701(47)
C(8)	2899(12)	1594(19)	−1334(10)	1309(122)	C(49)	5387(8)	−1761(13)	503(8)	761(53)
C(9)	3737(11)	−940(17)	−133(11)	1294(117)	C(50)	5438(7)	−2653(14)	200(8)	746(50)
C(10)	3994(10)	−1305(15)	−704(9)	1034(92)	C(51)	5067(9)	−3455(15)	347(9)	892(59)
C(11)	1915(6)	−1948(10)	3041(7)	479(38)	C(52)	4663(7)	−3383(12)	850(8)	658(46)
C(12)	2325(8)	−2569(14)	2761(8)	794(54)	C(53)	3769(6)	−3522(10)	1931(6)	442(36)
C(13)	2207(10)	−3644(16)	2790(10)	1013(67)	C(54)	4025(7)	−4035(12)	2455(7)	612(44)
C(14)	1731(9)	−3971(15)	3126(10)	907(61)	C(55)	3841(7)	−5033(12)	2575(8)	705(48)
C(15)	1335(10)	−3364(16)	3393(10)	1030(67)	C(56)	3388(7)	−5461(12)	2171(8)	688(47)
C(16)	1427(8)	−2304(13)	3380(8)	727(49)	C(57)	3133(7)	−4963(12)	1618(7)	609(43)
C(17)	1364(6)	−38(10)	3220(7)	476(37)	C(58)	3310(7)	−3950(11)	1524(7)	556(41)
C(18)	945(7)	210(11)	2756(7)	603(42)	C(59)	4452(6)	−1804(10)	2431(7)	488(38)
C(19)	377(7)	624(12)	2886(8)	683(48)	C(60)	4189(7)	−1071(12)	2811(8)	656(46)
C(20)	267(9)	786(14)	3523(9)	882(58)	C(61)	4516(8)	−727(13)	3350(8)	768(52)
C(21)	665(9)	566(15)	3999(10)	990(64)	C(62)	5095(8)	−1130(13)	3521(8)	793(52)
C(22)	1230(9)	112(14)	3858(9)	859(57)	C(63)	5335(7)	−1852(12)	3154(8)	677(47)
C(23)	2626(6)	−423(11)	3690(7)	476(38)	C(64)	5055(7)	−2213(12)	2593(7)	596(43)
C(24)	2806(8)	568(13)	3801(8)	737(51)					

[a] Defined as one-third of the trace of the orthogonalized $\mathbf{U}_{ij}$ tensor.

4.20−3.60 (complex, 8H, OCH_2), 1.72 (qn, $J_{HH} = J_{PH} = 7$, 6H, PCH_2), 1.28−1.00 (complex, 21H, Me).

Preparation of $[Mn_2Au_2\{\mu\text{-}P(OEt)_2\}\{\mu\text{-}\eta^2\text{-}OP(OEt)_2\}(CO)_6(PPh_3)_2]$ (6). A tetrahydrofuran solution (10 mL) containing 0.1 mmol of **1** was added into a Schlenk flask containing $[AuCl(PPh_3)]$ (0.099 g, 0.2 mmol) at −20 °C, and the mixture was stirred for 10 min and then concentrated under vacuum to *ca*. 2 mL. Toluene (20 mL) was then added, and the mixture was concentrated again to *ca*. 10 mL and further stirred for 30 min at room temperature to yield a dark red solution. Solvent was then removed under vacuum, the residue was extracted with toluene (15 mL), and this solution was filtered. Evaporation of the solvent from the latter solution and washing of the residue with petroleum ether (5 × 3 mL) gave compound **6** as an analytically pure red powder (0.109 g, 75%). Attempts to crystallize compound **6** from toluene/petroleum ether or dichloromethane/petroleum ether mixtures at −20 °C resulted in progressive decomposition of the complex. Anal. Calcd for $C_{50}H_{50}Au_2Mn_2O_{11}P_4$: C, 41.28; H, 3.46. Found: C, 41.59; H, 3.54. ^{1}H NMR (CD_2Cl_2): δ 7.64−6.98 (m, 30H, Ph), 4.51−4.14 (complex, 4H, OCH_2), 3.67−3.16 (complex, 4H, OCH_2), 1.48, 1.26, 1.07, 0.47 (4 × t, $J_{HH} = 7$, 12H, Me).

Preparation of $[Mn_2Ag_2\{\mu\text{-}P(OEt)_2\}\{\mu\text{-}\eta^2\text{-}OP(OEt)_2\}(CO)_6(PPh_3)_2]$ (7). By the procedure described for **6**, but using $[AgCl(PPh_3)]_4$ (0.044 g, 0.2 mequiv) and keeping the reaction mixture below 0 °C instead, compound **7** was isolated as an essentially pure red powder (0.092 g, 72%). Complex **7** has a low stability in solution at room temperature. Attempts to crystallize this species from toluene/petroleum ether mixtures at −20 °C also resulted in its progressive decomposition. Anal. Calcd for $C_{50}H_{50}Ag_2Mn_2O_{11}P_4$: C, 47.05; H, 3.95. Found: C, 46.66; H, 4.04. ^{1}H NMR (CD_2Cl_2, 263 K): δ 7.60−7.10 (m, 30H, Ph), 4.40−3.30 (complex, 8H, OCH_2), 1.44, 1.24, 1.12, 0.57 (4 × t, $J_{HH} = 7$, 12H, Me).

Preparation of $[Mn_2Au_3\{\mu\text{-}P(OEt)_2\}(CO)_6(PPh_3)_3]$ (8a). A toluene solution of compound **6** was prepared "in situ" as described above, but with a tetrahydrofuran solution containing 0.065 mmol of **1** and 0.196 mmol (0.097 g) of $[AuCl(PPh_3)]$ as starting material. Alumina (activity I, ca. 1 g) was then added, and the mixture was stirred at room temperature for 1 day to give a dark greenish mixture. Solvent was then removed under vacuum and the residue extracted with petroleum ether (5 × 3 mL) and chromatographed on alumina (activity III, 20 × 1.5 cm). Elution with dichloromethane/petroleum ether (1/3) gave a blue fraction which yielded, after removal of solvent under vacuum, compound **8a** as a blue microcrystalline solid (0.015 g, 11%). The crystals used in the X-ray study were grown by slow diffusion of a dichloromethane solution of **8a** into a layer of petroleum ether, at room temperature. Anal. Calcd for $C_{64}H_{55}Au_3Mn_2O_8P_4$: C, 43.26; H, 3.12. Found: C, 42.65; H, 3.02. ^{1}H NMR (C_6D_6): δ 7.98−7.92 (m, 6H, Ph), 7.25−7.15 (m, 9H, Ph), 6.97−6.80 (m, 30H, Ph), 4.77 (qn, $J_{HH} = J_{PH} = 7$, 4H, OCH_2), 1.34 (t, $J_{PH} = 7$, 6H, Me).

Preparation of $[Mn_2Au_3\{\mu\text{-}P(OEt)_2\}(CO)_6(PEt_3)_3]$ (8b). By the procedure described for **8a**, but starting with 0.05 mmol of **1** and 0.15 mmol (0.053 g) of $[AuCl(PEt_3)]$ instead, compound

8b was isolated as a blue microcrystalline solid (0.015 g, 15%). Anal. Calcd for $C_{28}H_{55}Au_3Mn_2O_8P_4$: C, 25.49; H, 3.95. Found: C, 25.02; H, 4.12. ^{1}H NMR (C_6D_6): δ 4.96 (qn, $J_{HH} = J_{PH} = 7$, 4H, OCH_2), 2.05 (qn, $J_{HH} = J_{PH} = 7.5$, 6H, PCH_2), 1.59 (t, $J_{HH} = 7$, 6H, OCH_2CH_3), 1.34 (dt, $J_{PH} = 16$, $J_{HH} = 7.5$, 9H, PCH_2CH_3), 0.94 (qn, $J_{HH} = J_{PH} = 7.5$, 12H, PCH_2), 0.66 (dt, $J_{PH} = 16$, $J_{HH} = 7.5$, 18H, PCH_2CH_3).

X-ray Data Collection, Structure Determination, and Refinement for Compounds 2 and 8a. The crystallographic data for both compounds are summarized in Table 6. Data were collected at room temperature (22 °C) on a Siemens AED (**2**) and a Philips 1100 PW (**8a**) diffractometer, using niobium-filtered (**2**) and graphite-monochromated (**8a**) Mo Kα radiation and the $\theta/2\theta$ scan type. The reflections for both **2** and **8a** were collected with a variable scan speed of 3−12° min^{-1} and a scan width of (1.20 + 0.346 tan θ)°. One standard reflection was monitored every 100 measurements; no significant decay was noticed over the time of data collection. The individual profiles have been analyzed following the method of Lehmann and Larsen.[32] Intensities were corrected for Lorentz and polarization effects. A correction for absorption was applied only to **8a** (maximum and minimum values for the transmission coefficients were 1.222 and 0.861).[33] Only the observed reflections were used in the structure solutions and refinements.

Both structures were solved by Patterson and Fourier methods and refined by full-matrix least squares, first with isotropic thermal parameters and then with anisotropic thermal parameters for the non-hydrogen atoms, except for the carbons of the ethyl groups (**2**) and of the phenyl groups (**8a**). All hydrogen atoms were placed at their geometrically calculated positions (C−H = 0.96 Å). The final cycles of refinement were carried out on the basis of 339 (**2**) and 460 (**8a**) variables. The highest remaining peak in the final difference map was equivalent to about 0.54 (**2**) and 0.86 (**8a**) e/Å^3. In the final cycles of refinement the weighting scheme $w = [\sigma^2(F_o)]^{-1}$ was used. The analytical scattering factors, corrected for the real and imaginary parts of anomalous dispersion, were taken from ref 34. All calculations were carried out on the Gould Powernode 6040 of the "Centro di Studio per la Strutturistica Diffrattometrica" del CNR, Parma, Italy, using the SHELX-76 and SHELXS-86 systems of crystallographic computer programs.[35] The final atomic coordinates for the non-hydrogen atoms are given in Tables 7 (**2**) and 8 (**8a**). The atomic coordinates of the hydrogen atoms are given in Tables SI (**2**) and SII (**8a**) and the thermal parameters in Tables SIII (**2**) and SIV (**8a**). (Tables SI−SIV are given in the Supporting Information).

Acknowledgment. We thank the Ministerio de Educación y Ciencia of Spain for a grant (to X.-Y.L.) and the DGICYT of Spain (Project PB91-0678) and Consiglio Nazionale delle Ricerche (Rome) for financial support.

Supporting Information Available: Hydrogen atom coordinates (Tables SI and SII), thermal parameters for the non-hydrogen atoms (Tables SIII and SIV), and all bond distances and angles (Tables SV and SVI) (16 pages). Ordering information is given on any current masthead page.

OM950604P

(32) Lehmann, M. S.; Larsen, F. K. *Acta Crystallogr., Sect. A* **1974**, *30*, 580.

(33) Walker, N.; Stuart, D. *Acta Crystallogr., Sect. A* **1983**, *39*, 158. Ugozzoli, F. *Comput. Chem.* **1987**, *11*, 109.

(34) *International Tables for X-Ray Crystallography*; Kynoch Press: Birmingham, U.K., 1974; Vol. IV.

(35) Sheldrick, G. M. SHELX-76 Program for Crystal Structure Determination; University of Cambridge, Cambridge, U.K., 1976; SHELXS-86 Program for the Solution of Crystal Structures; University of Göttingen, Göttingen, Germany, 1986.